Functional characterisation of rare variants in genes encoding the MAPK/ERK signalling pathway identified in long-lived Leiden Longevity Study participants

Helena Hinterding[1], Maarouf Baghdadi[1], Thies Gehrmann[2,3], Pasquale Putter[2], Nico Lakenberg[2], Erik B. van den Akker[2,3,4], P. Eline Slagboom[1,2*], Joris Deelen[1,5*#], Linda Partridge[1,6*#]

[1] Max Planck Institute for Biology of Ageing, Cologne, Germany

[2] Molecular Epidemiology, Department of Biomedical Data Sciences, Leiden University Medical Center, Leiden, The Netherlands

[3] Leiden Computational Biology Center, Leiden, The Netherlands.

[4] Delft Bioinformatics Lab, Delft University of Technology, Delft, The Netherlands.

[5] Cologne Excellence Cluster on Cellular Stress Responses in Ageing-Associated Diseases (CECAD), University of Cologne, Cologne, Germany

[6] Institute of Healthy Ageing, Department of Genetics, Evolution and Environment, University College London, London, UK

* These authors contributed equally to this study.

[#] Corresponding authors

Joris Deelen: Joris.Deelen@age.mpg.de

Linda Partridge: linda.partridge@ucl.ac.uk

Key words: MAPK/ERK signalling pathway, genetics, rare variants, longevity, ageing, functional characterisation, genome editing.

Abstract

Human longevity, which is coupled to a compression of age-related diseases, has been shown to be heritable. However, the number of identified common genetic variants linked to this trait remains small. This may indicate that longevity is, at least to some extent, determined by rare genetic variants that are potentially even family-specific. We therefore investigated whole-genome sequencing data of long-lived families from the Leiden Longevity Study for family-specific variants. We focussed on variants residing in genes involved in the MAPK/ERK signalling pathway, a lifespan-associated pathway emerging from studies in model organisms. We then used CRISPR/Cas9 to generate transgenic mouse embryonic stem cells (mESCs) and fruit flies harbouring these variants and conducted *in vitro* and *in vivo* functional characterisation. Two variants, located in *NF1* and *RAF1*, show opposite effects on MAPK/ERK signalling pathway activity in mESCs. At the proteomic level, we observed prominent changes that are shared between the variants (e.g. upregulation of the PI3K-AKT signalling pathway) and RAF1-specific (e.g. downregulation of oxidative phosphorylation). The variant in *RAF1* also improved resistance to endoplasmic reticulum and oxidative stress *in vitro*. Conversely, the variant in *NF1* shortened lifespan when introduced in fruit flies. In conclusion, our findings suggest that mESCs offer a good starting point for *in vitro* characterisation of rare genetic variants linked to human longevity. However, given the complex regulation of the MAPK/ERK signalling pathway across tissues and organisms and the large evolutionary distance between flies and humans, future studies will likely benefit from functional characterisation in human cells and model organisms evolutionary closer to humans.

Introduction

Human ageing is a complex trait influenced by many different factors, including genes, lifestyle, environmental circumstances, and access to healthcare [1]. Mainly due to advances in targeting the environmental component (through nutrition, hygiene, and medicine), human lifespan has greatly increased in the past two centuries [2]. However, there has thus far not been a similar increase in healthspan, i.e. the number of years lived before the occurrence of the first chronic disease [3]. There is therefore a growing period of loss of function and morbidity at the end of life, especially in women. Long-lived individuals, especially those from long-lived families, could offer mechanistic insights into how to improve late-life health, as they exhibit a compression of age-associated morbidity [4,5]. The longevity trait, defined as the capacity to reach exceptionally old ages (e.g. >90 years), is transmitted across generations in families where many members show a lifelong excess survival up to extreme ages despite sources of extrinsic mortality, such as epidemics, famine, or conflicts in the past two centuries [6–10]. This is exemplified by data from the Leiden Longevity Study (LLS) [11], which showed that individuals from long-lived families display beneficial immune and metabolic profiles in middle age [12–14]. Moreover, the long-lived siblings of this two generational-cohort provide a robust sample of individuals with an enrichment of the heritable component of longevity [15]. Therefore, we used data from these families to identify genetic variation that may contribute to mechanisms of late-life health.

Methods for identifying genetic variants associated with human longevity have thus far mainly focused on common variants using a population-based approach. This approach, including a global genome-wide association study (GWAS) [16], revealed a handful of loci associated with longevity, of which only *APOE* and *FOXO3* were consistently identified across epidemiological and family-based studies of ancestrally diverse populations [16–18]. Given the sparse findings from the GWAS approach, we instead focussed on rare variants with potentially larger effects that are not tagged by genome-wide genotyping arrays [19]. Unlike the hypothesis-free GWAS approach, which aims to identify common genetic variants across the genome associated with a trait in humans, the candidate-gene approach is applied to examine how a specific biological pathway relates to the trait under investigation [20]. Using this approach, and under the assumption that some longevity genes may be evolutionary conserved, several groups

have already started investigations in humans of lifespan-associated pathways and genes identified in model organisms [21–25].

We specifically investigated the MAPK/ERK signalling pathway because both genetic and pharmacological inhibition of its activity have been shown to extend lifespan in yeast, worms, flies, and mice [26–30]. MAPK/ERK signalling is well known for its key role in cell proliferation, survival, and metabolism [31,32]. Within this pathway, the activated RAS proteins function as central signalling hubs that initiate a downstream phosphorylation cascade through RAF, MEK, and, finally, ERK proteins, transmitting extracellular cues to the cytoplasm and, through the nuclear translocation of ERK, to the nucleus [26].

To study the role of genetic variation in the MAPK/ERK signalling pathway in modulating human longevity, we employed a heterologous systems approach to investigate the functional effects of rare protein-altering variants (with a minor allele frequency (MAF) below 0.01% in the general population) observed in the genome of long-lived individuals from the LLS [33]. We measured their effects on ERK1/2 phosphorylation, stress resistance, and protein abundance (i.e. proteomics) in mouse embryonic stem cells (mESCs). We subsequently generated fruit flies harbouring one of the conserved variants to functionally characterise whole organism-based phenotypes that cannot be evaluated using cellular models, such as lifespan. Notably, we observed that two variants, located in *NF1* and *RAF1*, showed opposite effects on MAPK/ERK signalling pathway activity (i.e. ERK1/2 phosphorylation) in mESCs, accompanied by prominent changes at the proteomic level, both shared between the variants (e.g. upregulation of the PI3K-AKT signalling pathway) and RAF1-specific (e.g. downregulation of oxidative phosphorylation). In addition, we found that the variant in *RAF1* improved resistance to endoplasmic reticulum (ER) and oxidative stress *in vitro*. Finally, our *in vivo* analyses showed that the homozygous (both sexes) and heterozygous (females only) mutant flies harbouring the variant in *NF1* were short-lived. Hence, although both the variant in *NF1* and *RAF1* show functional effects, our findings highlight the complex regulation of the MAPK/ERK signalling pathway at both the cellular and organismal level, thus complicating the interpretation of these effects in light of human longevity.

Results

Identification of rare protein-altering variants in genes involved in the MAPK/ERK signalling pathway in long-lived families from the LLS

To investigate whether genetic variation in the MAPK/ERK signalling pathway plays a role in human longevity, we focused on rare variants detected in whole-genome sequencing (WGS) data of long-lived individuals from the LLS [32]. The LLS cohort includes two generations of family members from 421 families selected based on long-lived siblings living in the Netherlands at the time of inclusion (men aged 89 years or above; women aged 91 years or above) [34]. For the purpose of this study, we focused on the parental generation of the LLS and, more explicitly, the families who showed the strongest evidence for familial genetic enrichment of longevity, as previously defined by van den Berg and colleagues [15]. This means that at least two siblings within the family belonged to the top 10% longest-lived of their birth cohort and had a parent meeting the same criterion [15]. Of the 216 remaining families, we focussed on the subset of 183 unrelated individuals from these families for whom WGS data was available. The mean age at death of these individuals is 98.2 years (standard deviation = 3.4 years). The genetic variants from the WGS data of the subset of individuals from long-lived families were subsequently filtered according to the following criteria (**Figure 1A**):

(1) The variant resides in the coding region of a MAPK/ERK signalling-related gene (see **Table EV1** for an overview of the used gene list).

(2) The variant is protein-altering with a combined annotation-dependent depletion (CADD v1.3) score ≥20 (i.e. belonging to the top 1% of variants in the genome that are most likely to affect protein function) [36,37].

(3) The variant is absent (MAF = 0%) in Dutch-specific controls (BBMRI-NL) [33,35] and is absent or has a very low frequency (MAF <0.01%) in the general population, as determined using the publicly available reference database gnomAD (ALL population) (https://gnomad.broadinstitute.org/ v.2.1.1.).

(4) The variant is located in a genomic region that is shared between long-lived family members (identity-by-descent (IBD) ≥1 based on Illumina BeadChip data).

(5) The variant is validated using Sanger sequencing in the sequenced individual, as well as at least one long-lived sibling from the same family, to increase the likelihood that the variant contributes to familial longevity.

In total, we identified 10 variants meeting these criteria (**Figure 1B** and **Table 1**).

Generation of mESCs harbouring the identified variants

To study the functional consequences of the identified variants, we performed CRISPR/Cas9 gene editing using the $Cas9^{D10A}$ nickase enzyme (double-nicking strategy) [36] to generate transgenic haploid AN3-12 mESCs [37]. Previous longevity interventions in the MAPK/ERK signalling pathway have focussed on genes upstream of ERK [37,38]. Therefore, we prioritised the variants located in genes upstream in the pathway and successfully generated mESC lines harbouring four of them, i.e. Ala1127Val and Phe1112Leu (for which we were able to generate two independent cell lines) in NF1, Asp633Tyr in RAF1, and Glu118Lys in RRAS (**Figure 2A-B** and **Figure EV1**, respectively).

MAPK/ERK signalling pathway activity of generated mESC lines

To assess changes in activity of the MAPK/ERK signalling pathway by western blotting, we used the ratio of phosphorylated (Thr202/Tyr204 ERK1 and Thr185/Tyr187 ERK2) over total ERK1/2 (p44/42 MAPK) [38–40]. This ratio was sufficiently high in diploid AN3-12 mESCs, when maintained in normal growth medium, to assess MAPK/ERK activity without the need to additionally activate the pathway. This is probably due to the high proliferative nature of these actively dividing stem cells. Therefore, we performed all subsequent experiments with diploid mESCs maintained in normal growth medium containing the variants of interest in the homozygous state.

The two independent mESC lines harbouring the $NF1^{Phe1112Leu}$ variant displayed a significant reduction in ERK1/2 phosphorylation (**Figure 2C**). This suggests a potential increase in NF1 activity, given previously reported elevations of pathway activity in *Nf1* knockout mouse embryonic fibroblasts (MEFs) and in brains of conditional neuronal knock-out mice [41,42]. In contrast, the mESC line harbouring the $RAF1^{Asp633Tyr}$ variant showed an increase in ERK1/2 phosphorylation (**Figure 2D**), suggesting a possible increase in RAF1 activity. Interestingly, human disease-causing gain-of-function mutations in RAF1 have also been reported to cause increased ERK1/2 phosphorylation when introduced into human cell lines [41,43]. The mESC lines harbouring the other variant located in the *NF1* gene, $NF1^{Ala1127Val}$, as well as the variant in RRAS, $RRAS^{Glu118Lys}$, showed no change in ERK1/2 phosphorylation (**Figure 2C** and **Figure EV1**). We therefore decided to not take these variants forward for further experiments.

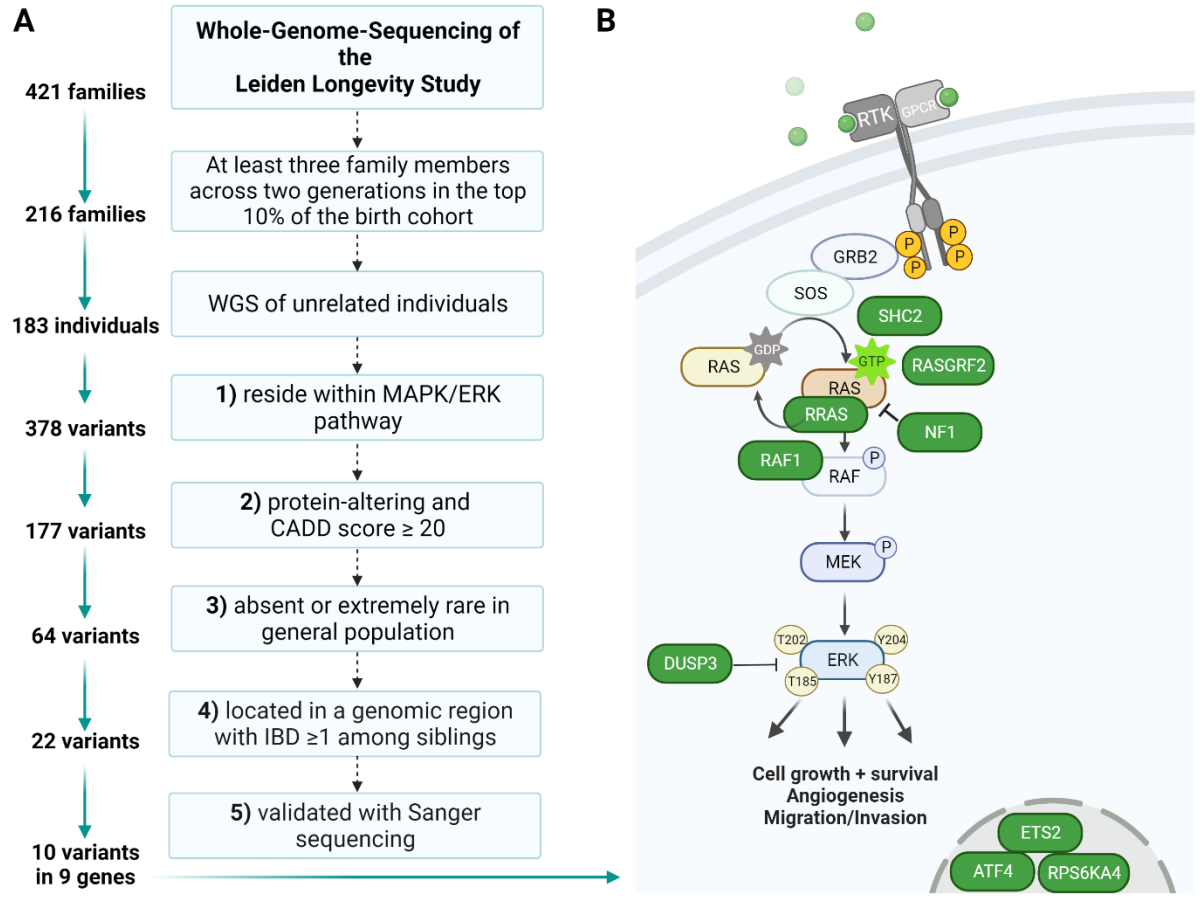

Figure 1 | Identification of MAPK/ERK signalling pathway-associated rare genetic variants in long-lived individuals

(A) Schematic of the pipeline used to filter the whole-genome-sequencing data of long-lived individuals from the Leiden Longevity Study. This filtering resulted in a list of 10 variants residing within 9 genes encoding the MAPK/ERK signalling pathway. **(B)** Simplified illustration of the MAPK/ERK signalling pathway with genes containing variants highlighted in green. The MAPK/ERK signalling pathway transmits cues into the cytoplasm and consists of upstream located RAS proteins and a phosphorylation cascade of RAF-, MEK-, and ERK-kinases. WGS; whole-genome sequencing, CADD; combined annotation-dependent depletion, IBD; identity-by-descent.

Table 1 | The 10 rare genetic variants in the MAPK/ERK signalling pathway identified in long-lived family members from the Leiden Longevity Study

Gene	Position	AA change in humans	AA change in mice	AA change in fruit flies	CADD score	Allele frequency in Europeans
DUSP3	17-41847063-G-A	Arg158Cys	Arg158Cys		35.0	0.004399%
RASGRF2	5-80369192-C-A	Leu270Ile	Leu270Ile		24.7	0%
ATF4	22-39918575-C-T	Arg342Cys	Arg340Cys		33.0	0.004537%
SHC2	19-436409-T-C	Tyr266Cys	Tyr244Cys		25.8	0%
RAF1	**3-12626063-C-A**	**Asp633Tyr**	**Asp633Tyr**	**Asp713Tyr**	**31.0**	**0**%
ETS2	21-40186295-C-T	Arg235Trp	Arg95Trp		23.5	0.002324%
RPS6KA4	11-64135713-C-T	Ala394Val	Ala394Val		23.2	0%
NF1	**17-29559777-C-T**	**Ala1125Val**	**Ala1127Val**		**22.0**	**0.0008796**%
NF1	**17-29559731-T-C**	**Phe1110Leu**	**Phe1112Leu**	**Phe1148Leu**	**27.9**	**0**%
RRAS	**19-50139977-C-T**	**Glu118Lys**	**Glu118Lys**	**Glu118Lys**	**35.0**	**0.006170%**

Variants found in genes highlighted in bold were generated in mouse embryonic stem cells and/or *Drosophila melanogaster*. The implicated amino acids of the variants in *NF1*, *RAF1*, and *RRAS* are conserved in the fruit fly. CADD; combined annotation dependent depletion, AA; amino acid. The position of the variants is based on the human assembly GRCh37 (hg19). Allele frequencies are based on high quality genotypes of Europeans (non-Finnish) who are included in the gnomAD database v2.1.1.

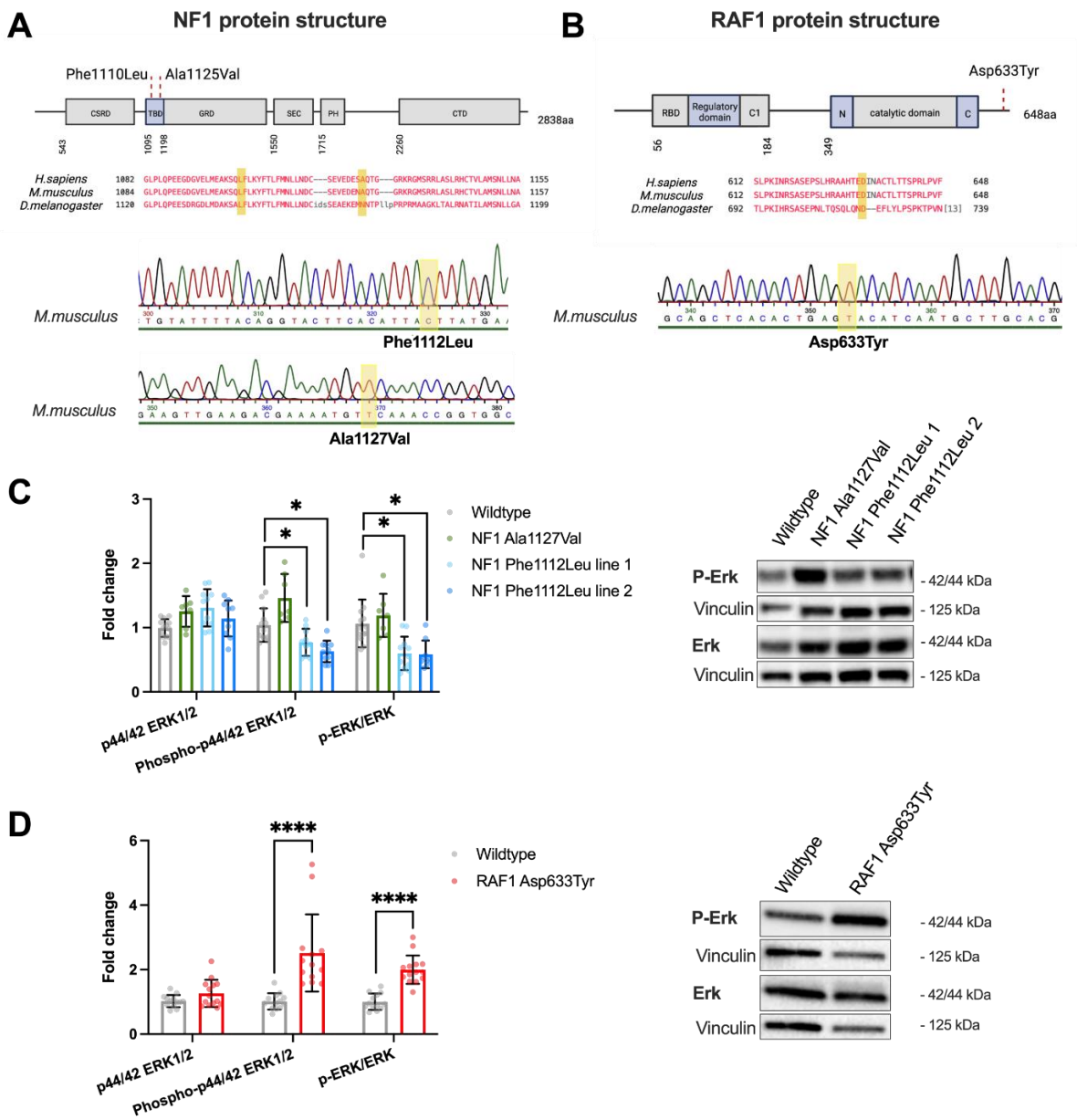

Figure 2 | The effect of the rare genetic variants in *NF1* and *RAF1* on MAPK/ERK signalling pathway activity

Schematic representation highlighting the features and domains of the (**A**) NF1 and (**B**) RAF1 proteins, including the location of the identified variants (denoted by dashed red lines), as well as the sequence homology between humans, mice, and flies, and the DNA sequence resulting from Sanger sequencing validation (with the mutation highlighted in yellow). MAPK/ERK signalling pathway activity, represented by the ratio of phosphorylated over total ERK (normalised to Vinculin), in the mESC lines harbouring **(C)** $NF1^{Ala1127Val}$ and $NF1^{Phe1112Leu}$ and **(D)** $RAF1^{Asp633Tyr}$. The data shown is from three pooled western blots. Dots represent technical replicates. Error bars represent standard deviation. Data was analysed using a two-sample Student's t-test. *P < 0.05, **P < 0.01, ***P < 0.001. CSRD; cysteine- and serine-rich domain, TBD; tubulin-binding domain, GRD; GAP-related domain, Sec; Sec14 homologous domain, PH; pleckstrin homology domain, CTD; C-terminal domain, RBD; Ras-binding-domain, C1; cysteine-rich domain, GTP; Guanosine triphosphate binding sites, ATP; Adenosine triphosphate binding sites.

Resistance to oxidative and endoplasmic reticulum stress

Previous studies have shown that the MAPK/ERK signalling pathway is activated in response to increased endoplasmic reticulum (ER) and oxidative stress to maintain survival [44–47]. In order to assess if the NF1^{Phe1112Leu} and RAF1^{Asp633Tyr} variants also altered these stress responses, we stressed the mESC lines harbouring them with tunicamycin (ER stress) and hydrogen peroxide (H_2O_2, oxidative stress). The two independent cell lines harbouring the NF1^{Phe1112Leu} variant did not differ from wildtype mESCs in their response to either tunicamycin- or H_2O_2-induced stress (**Figure 3A-B**). The RAF1^{Asp633Tyr} variant mESC line, on the other hand, showed a significantly increased resistance to both stressors (**Figure 3C-D**).

Proteomics of the NF1 and RAF1 mESC lines

The MAPK/ERK signalling pathway contains multiple positive and negative feedback loops, complicating the functional interpretation of single readouts of their activity. We therefore also assessed broader functional effects of the mutants. We performed LC-MS/MS-based TMT-labelled quantitative proteomics of the mESC lines harbouring the NF1^{Phe1112Leu} and RAF1^{Asp633Tyr} variants. In total, we were able to detect 7726 proteins. In line with the ERK1/2 phosphorylation data, principal component analysis confirmed that the two variants showed a distinct proteomic profile, with the two independent cell lines harbouring NF1^{Phe1112Leu} clustering together (**Figure EV2**). This also decreased the likelihood that the observed effects are caused by potential off-target effects inherent to genome editing. The overlap in differentially abundant proteins (DAPs) in the transgenic mESC lines were strongest upstream in the MAPK/ERK signalling pathway (**Figure 4A-B**), characterised by a significantly increased expression of EGFR and GRB2 and a decreased expression of RASGRP4. The NF1^{Phe1112Leu} and RAF1^{Asp633Tyr} proteomic profiles started to diverge at the level of the RAS protein family, exemplified by an increased expression of RRAS in the NF1^{Phe1112Leu} variant mESC line and a decreased expression in the RAF1^{Asp633Tyr} variant mESC line. The majority of the MAPK/ERK signalling pathway-specific DAPs in the RAF1^{Asp633Tyr} variant mESC line were downregulated, suggesting negative feedback from ERK1 to upstream located proteins. Interestingly, RAF1 itself was also downregulated in this mESC line, while NF1 was upregulated, indicative of an overall reduced activity of the MAPK/ERK signalling pathway.

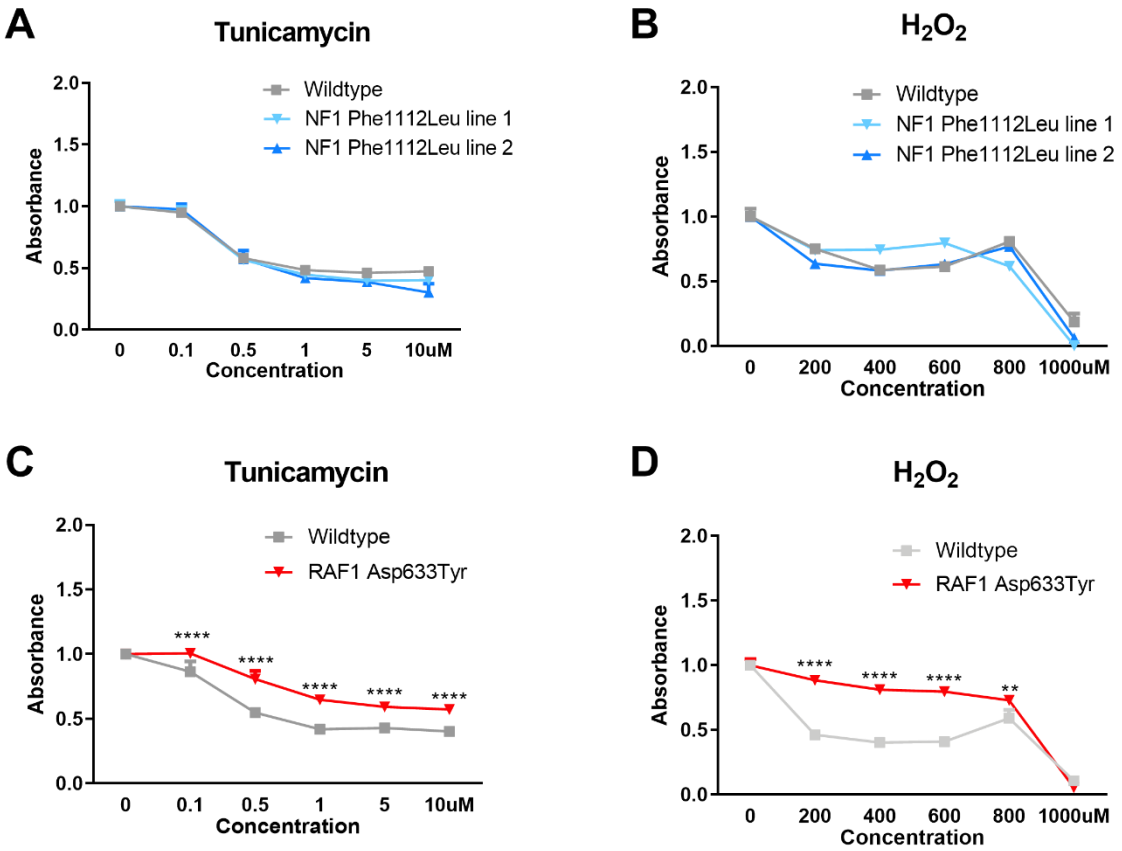

Figure 3 | The *Raf1*^{Asp633Tyr} variant improves stress resistance in mESCs

Survival of the NF1^{Phe1112Leu} variant mESC lines was not significantly different from wildtype mESCs in response to **(A)** ER stress (tunicamycin) or **(B)** oxidative stress (H_2O_2). The RAF1^{Asp633Tyr} variant mESC line showed significantly elevated stress resistance in response to **(C)** ER stress and (**D**) oxidative stress. Values were normalised to the respective untreated controls and analysed with a two-way ANOVA for each concentration. Error bars represent standard error of the mean (*n*=4). *P < 0.05, **P < 0.01, ***P < 0.001.

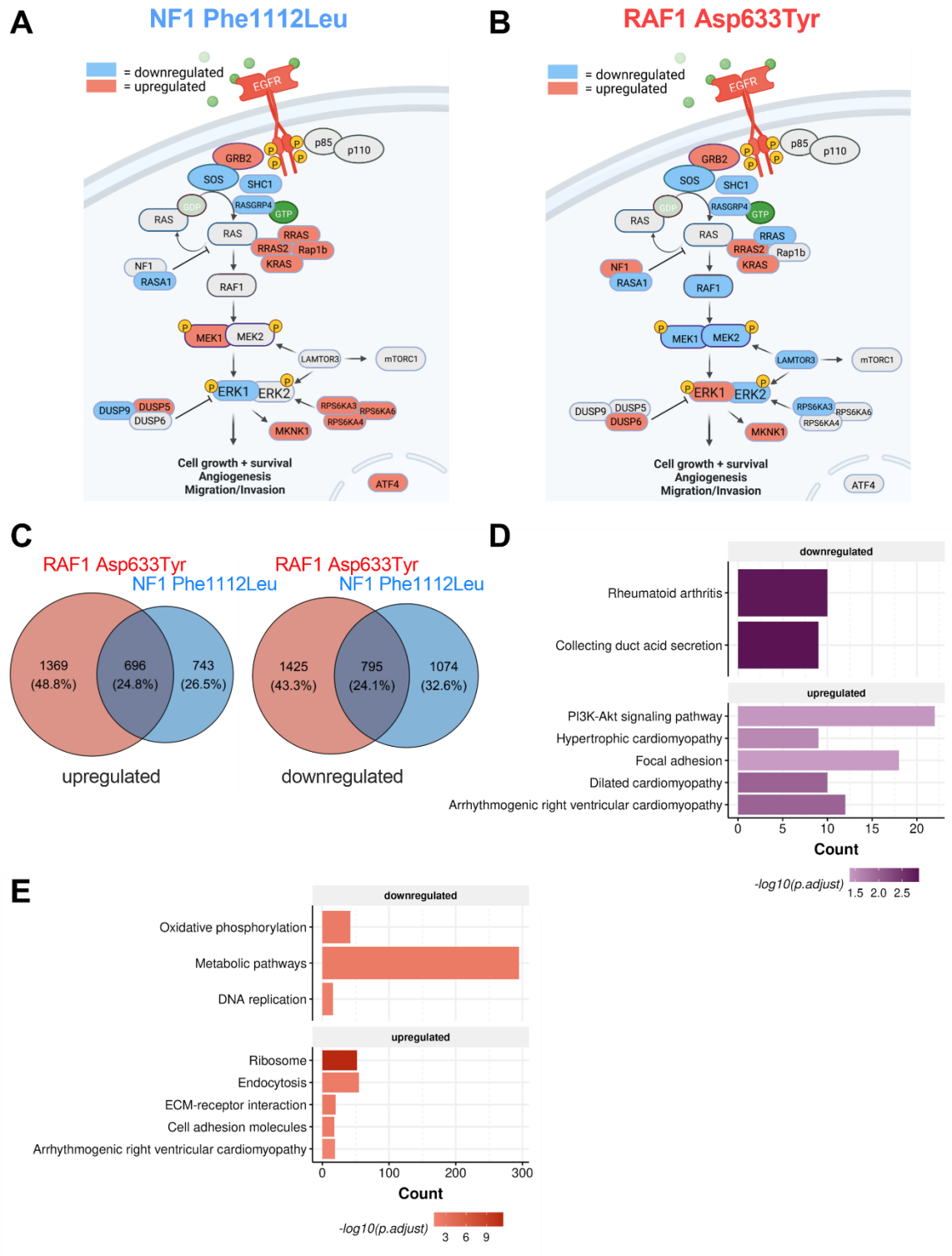

Figure 4 | Proteomics of the NF1^{Phe1112Leu} and RAF1^{Asp633Tyr} variant mESC lines

Differentially abundant proteins (DAPs) in the MAPK/ERK signalling pathway in the NF1^{Phe1112Leu} **(A)** and RAF1^{Asp633Tyr} variant mESC line **(B)** (red = significantly upregulated DAPs; blue = significantly downregulated DAPs). **(C)** Venn diagrams representing the number and proportion of up- and down-regulated proteins in the NF1^{Phe1112Leu} and RAF1^{Asp633Tyr} variant mESC lines. **(D)** Overrepresentation analysis using KEGG pathways for DAPs that are shared between NF1^{Phe1112Leu} and RAF1^{Asp633Tyr} variant mESC lines. **(E)** Overrepresentation analysis using KEGG pathways for RAF1^{Asp633Tyr}-specific DAPs.

To probe effects of the variants on broader biological processes, we performed overrepresentation analysis using KEGG pathways on the shared and cell line-specific DAPs of the NF1^{Phe1112Leu} and RAF1^{Asp633Tyr} variant mESC lines (**Figure 4C**). Shared upregulated DAPs showed an enrichment of several pathways, including the PI3K-AKT signalling pathway (**Figure 4D** and **Table EV2**), which shares growth factor activated receptors and transcription factors with the MAPK/ERK signalling pathway. For the RAF1^{Asp633Tyr}-specific downregulated DAPs, we detected strong enrichment of both oxidative phosphorylation and metabolic pathways, while the upregulated DAPs show the strongest enrichment for ribosome and endocytosis **(Figure 4E)**. For the NF1^{Phe1112Leu}-specific DAPS, we did not observe any significant enrichment.

Generation and characterisation of transgenic flies harbouring the Nf1^{Phe1112Leu} variant

Responses of individual cells to mutations are informative, but cannot provide information on the effects on a whole organism. We therefore assessed whether the *in vitro* effects of the variants were recapitulated *in vivo*. This also allowed us to study the effects of the mutations in both the heterozygous and homozygous state. Since the original amino acids containing the NF1 and RAF1 variants are conserved in *Drosophila melanogaster* (i.e. Nf1^{Phe1148Leu} and Raf^{Asp713Tyr}), we attempted to create transgenic fly lines harbouring these variants. We did not succeed in generating a transgenic Raf^{Asp713Tyr} fly line, probably because this variant leads to embryonic lethality. We were, however, able to generate a transgenic fly line harbouring the Nf1^{Phe1148Leu} variant (**Figure EV3A**), which we subsequently backcrossed for six generations into the *w^{Dah}* background. Overexpression of Nf1 in the fruit fly has been shown to extend lifespan, increase fecundity, and increase resistance to both oxidative and thermal stress [48]. We assessed ERK1/2 phosphorylation in male and female fly heads, where Nf1 is known to be highly expressed [49], but we did not observe any significant difference in MAPK/ERK signalling pathway activity in flies carrying the variant (**Figure 5A-B**). To determine if the Nf1^{Phe1148Leu} variant had an effect on lifespan, we used once-mated, heterozygous and homozygous transgenic flies of both sexes. Lifespan of homozygous Nf1^{Phe1148Leu} flies was significantly reduced compared to controls in both sexes, while survival of heterozygous flies was only significantly reduced in females (**Figure 5C-D** and **Figure EV4A-B**). These findings indicate that the Nf1^{Phe1148Leu} variant is deleterious to survival in the fruit fly.

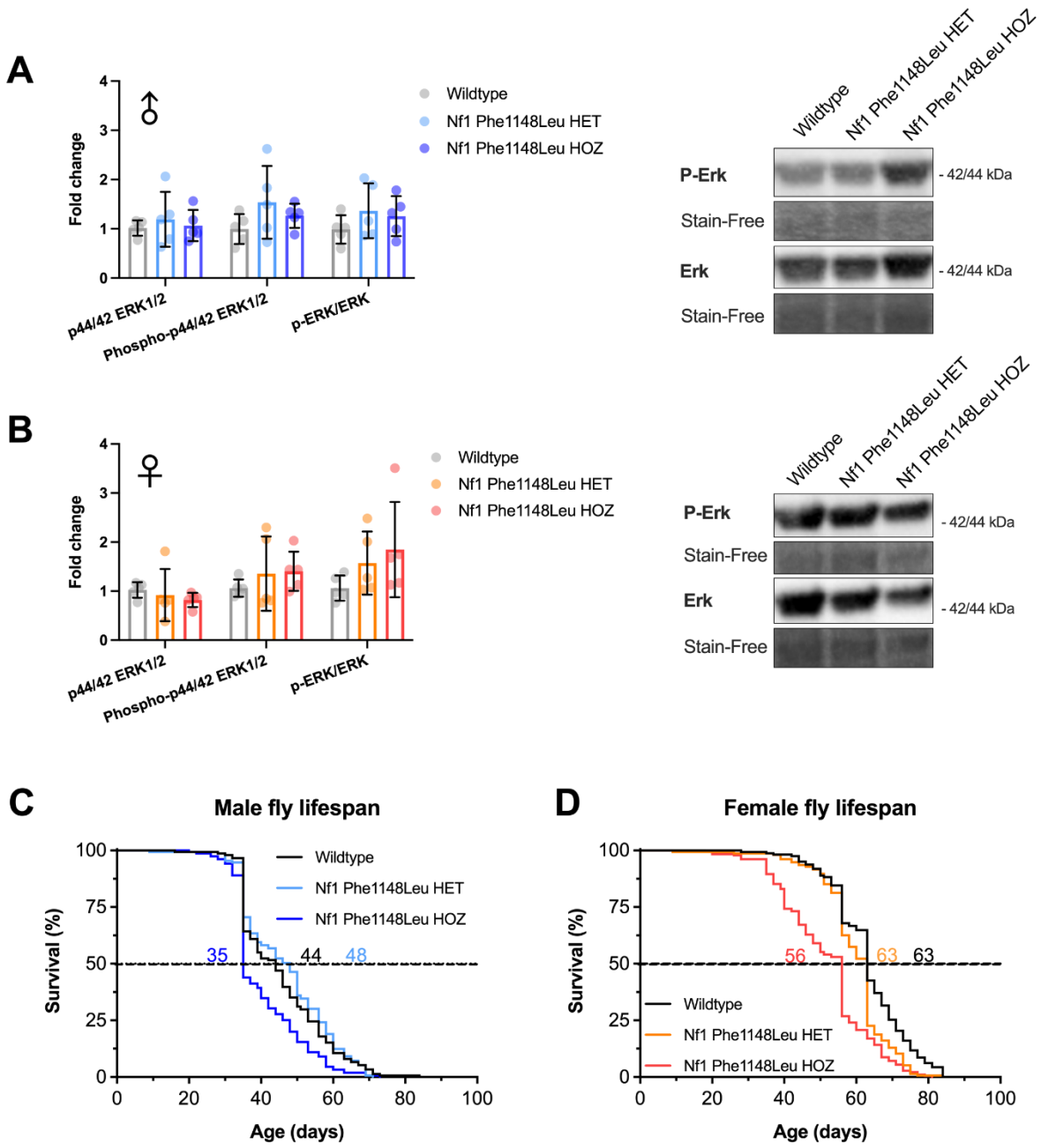

Figure 5 | The effect of the Nf1^{Phe1148Leu} variant on MAPK/ERK signalling pathway activity and lifespan
Western blotting showed no effect of the Nf1^{Phe1148Leu} variant on the ratio of phosphorylated over total ERK in male **(A)** or female flies **(B)**. The data shown is from two pooled western blots. The western blots were analysed with a one-way ANOVA and Dunnett's post hoc test. Dots represent technical replicates (n=25 per replicate). Error bars represent standard deviation. Arbitrary region of Stain-Free membrane (which leads to a fluorophore covalently bound to all proteins) was used to normalise the fold change of ERK and phospho-ERK. **(C-D)** Lifespan assay of wildtype, heterozygous, and homozygous Nf1^{Phe1148Leu} **(C)** male and **(D)** female flies. Data was analysed by both log-rank and Cox regression in which wildtype vs. Nf1^{Phe1148Leu} HET (females only) and wildtype vs. Nf1^{Phe1148Leu} HOZ (both sexes) were significant ($P < 0.001$) (n>150 flies per condition). HET; heterozygous, HOZ; homozygous. The raw lifespan data is provided in **Dataset EV1**.

We continued the functional characterization of the Nf1^{Phe1148Leu} flies and assessed body weight, developmental time, fecundity, and climbing ability. Female flies carrying the Nf1^{Phe1148Leu} variant in the homozygous state were significantly smaller than wildtype flies (**Figure EV3B**). Lifespan modulations in flies often occur at the expense of fecundity [50,51]. We therefore assessed fecundity, but did not observe any significant difference between Nf1^{Phe1148Leu} and wildtype flies (**Figure EV3C**). In heterozygous and homozygous flies carrying the Nf1^{Phe1148Leu} variant, we found a small, but significant, developmental delay of flies hatching from synchronised eggs (**Figure EV3D**). Next, we looked at climbing ability of adult transgenic flies, which is a commonly used read-out for locomotor activity and deteriorates with increasing age [21,52]. Male heterozygous Nf1^{Phe1148Leu} flies showed no significant difference in climbing ability across age, while there was a significant reduction in homozygous Nf1^{Phe1148Leu} compared to heterozygous and wildtype flies (**Figure EV3E**). Female heterozygous and homozygous Nf1^{Phe1148Leu} flies showed no significant reduction in climbing ability (**Figure EV3F**). The presence of the Nf1^{Phe1148Leu} variant in the homozygous state thus leads to a delay in development, reduced adult body size, and reduced locomotor activity in fruit flies.

Discussion

In this study, we present a novel pipeline for the functional characterisation and potential validation of rare genetic variants linked to human longevity. Transgenic cell lines and flies were generated using CRISPR/Cas9 gene editing to introduce four variants in three genes identified in long-lived family members from the LLS. The effects of these variants were assessed through cellular read-outs, such as ERK1/2 phosphorylation, stress resistance, and proteomic signatures. Two genetic variants, located in *NF1* (Phe1112Leu) and *RAF1* (Asp633Tyr), showed different effects on these cellular read-outs. Transgenic flies were generated for the NF1 variant, and the effect on complex phenotypes such as lifespan, climbing ability, and development was assessed. The results showed a significant reduction in lifespan of homozygous flies and a female-specific reduction in heterozygous flies. Additionally, there was a male-specific reduction in climbing ability of homozygous and heterozygous flies, and a significant delay in development of homozygous and heterozygous flies.

Genetic and pharmacological inhibition of the MAPK/ERK signalling pathway have been shown to extend lifespan in different organisms [51]. However, the activity of the MAPK/ERK signalling pathway appears to be differentially regulated in this context. On the one hand, reduced ERK signalling activity, by means of treatment with the MEK kinase inhibitor trametinib, results in lifespan extension in flies [53]. On the other hand, elevated ERK signalling activity in human lung and dermal fibroblasts, was shown to extend replicative lifespan [53]. These observations suggest that the effects of decreased or increased MAPK/ERK signalling activity on longevity may be cell- and/or tissue-type specific.

The elevated ERK1/2 phosphorylation in the RAF1^{Asp633Tyr} variant mESC line points towards a gain-of-function effect, as this gene is a known activator of the pathway. However, the proteomic analysis revealed that negative feedback from ERK1 could potentially have resulted in overall downregulation of proteins involved in the MAPK/ERK signalling pathway in this mESC line. Another possibility is that other RAF kinase family members (over-)compensate for a potential loss-of-function effect, as observed in MEFs of conditional *Raf1* knock-out mice, which do not show altered ERK1/2 phosphorylation [54–56]. Pathway enrichment analysis of the proteomic data of this variant further revealed reduced abundance of metabolic pathways and oxidative phosphorylation-related proteins. In worms, flies, and mice it has been shown that

mild inhibition of oxidative phosphorylation is one way to achieve lifespan extension [57–59]. In addition, RAF1^{Asp633Tyr} variant mESCs exhibited an improved response to different stressors, which has also been linked with improved lifespan and longevity [60–63]. Follow-up experiments of this variant *in vivo* should be performed to determine whether model organisms harbouring this variant indeed present an improved stress response and increased longevity.

Given the role of NF1 as an inhibitor of the MAPK/ERK signalling pathway, reduced ERK1/2 phosphorylation in the NF1^{Phe1112Leu} variant mESC line points towards a gain-of-function effect. However, proteomic analysis revealed an overall elevated expression of MAPK/ERK signalling-related DAPs and no effect on NF1 itself. Successful introduction of this variant in the fruit fly did not result in a significant difference in ERK1/2 phosphorylation in heterozygous nor homozygous Nf1^{Phe1148Leu} flies. However, since we only tested fly heads, it could still be that MAPK/ERK signalling is altered in other tissues. Moreover, Nf1^{Phe1148Leu} flies showed reduced lifespan in the homozygous (both sexes) and heterozygous state (female-specific). One study has reported that through the adenylyl cyclase/cAMP/PKA pathway, Nf1 deficiency can result in reduced lifespan, while Nf1 overexpression can lead to increased lifespan in flies [64]. Based on these findings, we propose that the NF1^{Phe1112Leu} variant likely results in a loss-of-function of Nf1 in flies *in vivo*, resulting in a detrimental effect on lifespan, potentially through the adenylyl cyclase/cAMP/PKA pathway. In line with previous findings, we observed differential regulation of MAPK/ERK signalling pathway activity in different model systems, i.e. mESCs and fruit flies, which raises the question if these models can be used to study human variants. Further studies are needed to determine if similar effects are observed in higher organisms, such as mice, and if the NF1^{Phe1112Leu} variant may still have longevity-promoting effects in humans.

Stem cells are a commonly used cell line in biomedical research because of their unlimited capacity to divide and differentiate into different cell types [65]. In this study, we opted for AN3-12 mESCs given that these cells have successfully been used for CRISPR/Cas9 genome engineering in previous studies [66]. This mESC line provides a valuable tool for functional genomics, as it allows for precise genome editing in the haploid state and does not possess karyotypic abnormalities, such as polyploidy, that could affect functional characterisation. Haploid mESCs can be edited more efficiently because targeted mutagenesis in diploid cell lines often results in unwanted insertions or deletions on at least one of the targeted alleles [67]. Haploid mESCs naturally become diploid over time so, after the mutations had been

introduced, we were able to select the diploid mESCs in which we studied the functional effects of the mutations in the homozygous state. However, a limitation of this approach is that the variants found in long-lived individuals were identified in the heterozygous state. As we expected potential mild functional effects, we aimed to increase their functionality by first generating homozygous cell lines that contain two alleles rather than one. Future studies should investigate the $RAF1^{Asp633Tyr}$ variant in the heterozygous state in both mouse and human cell lines, ideally obtained from carriers of the variants. Moreover, although cellular models offer a good starting point for functional characterisation, longevity studies of conserved variants should be conducted in model organisms, such as worms, flies, and/or mice to be able to determine their more complex *in vivo* effects. We also attempted this in this study using fruit flies, but with limited success. This may be explained by the evolutionary distance between species and context-dependent regulation of the MAPK/ERK signalling pathway that also differs in terms of its complexity between species.

Another limitation of our approach is that studies of rare variants are limited by statistical power [68]. With this approach, a common issue faced by researchers is the inability to prove functionality and statistically significant enrichment in humans. Strikingly, in our study, the two variants that showed functional effects on MAPK/ERK signalling pathway activity, $RAF1^{Asp633Tyr}$ and $NF1^{Phe1112Leu}$ are shared among long-lived family members, but are completely absent in the public reference database gnomAD (https://gnomad.broadinstitute.org/) and Dutch-specific controls [33,35], which may indicate that familial sharing of these alleles is less likely a chance finding. However, it remains unclear whether these variants contribute to the longevity of their carriers. Other groups have used similar approaches, but focussed on variants identified in individuals without a known family history for longevity that were often also observed in control populations (sometimes even at a similar frequency). Although some of these variants also show functional effects in cell lines, it is perhaps even less likely that they contribute to longevity of their carriers, given that most of the controls will not reach an exceptionally old age [68]. We therefore suggest that future functional studies of genetic variants should focus on genetic variants uniquely identified in, and ideally shared by, long-lived individuals within families.

In conclusion, we have created a pipeline for the identification and functional characterisation of rare genetic variants discovered in families enriched for longevity. We successfully applied this pipeline to determine the functional effects of genetic variation in the MAPK/ERK

signalling pathway in different model systems. We believe this approach can also be applied to functionally characterise variants associated with other complex traits. Our results suggest that cellular models offer a good starting point for functional characterisation. However, in order to understand how MAPK/ERK signalling-related genetic variation may contribute to longevity *in vivo*, model organisms evolutionary closer to humans, such as mice, will have to be studied given the observed differential regulation of this pathway across species.

Methods

Study populations and selection criteria

The population used in this study has already been described previously [69]. In brief, we utilised WGS data of 183 families belonging to the LLS. The LLS consists of Dutch families with at least two siblings meetings the following inclusion criteria: (1) men and women are at least 89 and 91 years old respectively, (2) participants have at least one living sibling who fulfils the first criterion, (3) the nonagenarian sibship share the same mother and father, and (4) the parents of the nonagenarian sibship are from European ancestry. For the purpose of this study, we applied a number of filters (see **Figure 1A**) to the WGS data of these nonagenarians, for which genetic variants were annotated with the Ensembl Variant Effect Predictor using the human assembly GRCh37 (hg19) as reference [70,71]. To determine the frequency of the identified rare protein-altering variants in a background population similar to our long-lived individuals, we utilised sequencing data from 100 individuals of Dutch Caucasian origin (<=65 years old) collected by the Dutch Biobanking and Biomolecular Resources Research Infrastructure initiative (BBMRI-NL) [35]. These individuals were not selected for particular characteristics other than that they should reflect a random sample of the apparently healthy Dutch population. The IBD between long-lived family members was calculated using the --ibd module from Merlin using previously generated genome-wide genetic data from Illumina BeadChips [72].

Genotyping

For standard genotyping of mouse embryonic stem cells (mESCs), GoTaq Master Mixes (Promega, Wisconsin, United States) were used according to manufacturer's instructions. For standard genotyping of fruit flies, HotStarTaq Plus MasterMix (Qiagen, Germany) was used according to manufacturer's instructions. Oligonucleotides (**Table EV3**) were ordered from Sigma-Aldrich. To analyse the size of DNA fragments or plasmids, 1x or 2x TAE (Tris base, acetic acid, ethylenediaminetetraacetic acid; Promega) buffered agarose gel electrophoresis was used to separate DNA. DNA was stained with 10 µL Gel Red Stain (Invitrogen, Massachusetts, United States) per 100 mL agarose gel. Electrophoresis was performed with the Sub Cell GT horizontal electrophoresis system (BioRad, California, United States) for 30-60 min at 60-130 V. Hyperladder 50 bp or Hyperladder 1 kb (Bioline) served as DNA fragment size markers.

Cloning

Guide RNAs (gRNAs) targeting the desired locus (**Table EV4**) were designed with Benchling (https://www.benchling.com) and ordered from Sigma-Aldrich (Missouri, United States). For cloning, Phusion High Fidelity Master Mix with GC Buffer (NEB, Massachusetts, United States) was used. All restriction digest reactions were performed with enzymes provided by NEB according to manufacturer's instructions. T4 DNA Ligase (NEB) was used for ligation reactions. Two gRNAs were independently cloned into a vector containing the $Cas9^{D10A}$ nickase enzyme (pSpCas9n(BB)-2A-GFP) (PX461), to minimise off target mutagenesis [72]. pSpCas9n(BB)-2A-GFP (PX461) was a gift from Feng Zhang (Addgene plasmid #48140; https://www.addgene.org/48140/; RRID:Addgene_48140). Chemically competent OneShot TOP10 *Escherichia coli* (LifeTechnologies) were used for transformation of ligation reactions or plasmids according to manufacturer's instructions. For positive selection of transformants, a 100 µg/mL ampicillin in Luria-Bertani (LB) plates were used. LB medium contained 5 g yeast extract, 10 g tryptone, 10 g NaCl 10 g (Sigma), and 1 l deionized water. The solution was adjusted to pH 7.0 and autoclaved before usage. For subsequent plasmid purification from bacteria, the QIAprep Miniprep or Midiprep Kits (Qiagen) were used. Cloning success was verified with Sanger Sequencing at Eurofins Genomics (Germany).

Cell culture

mESCs

AN3-12 mESCs were generated previously [37]. They were cultured in high glucose Dulbecco's Modified Eagle Medium supplemented with 3.7 g/l Sodium bicarbonate, 13.7% FBS, 1% Pen-Strep, 1% L-Glutamate, 1% Sodium Pyruvate, 1% MEM Non-Essential amino acids, 0.1% beta-mercaptoethanol and 0.01% leukaemia inhibitory factor (Millipore, Massachusetts, United States). Cells were grown in petri dishes as semi-adherent colonies at 37°C with 5% CO2.

CRISPR/Cas9 plasmid transfection

The created gRNA-containing vectors were subsequently transfected into the wildtype mESCs using Lipofectamine 3000 (Thermo Fisher, Massachusetts, United States) together with a short (~120 bp) single-stranded DNA oligonucleotide (ssODN) (**Table EV5**). The ssODN contained the mutation of interest, as well as a minimum of two silent mutations. One silent mutation in

the protospacer adjacent motif (PAM) that prevents the Cas9n protein from re-cutting after successful repair as well as one mutation to add a restriction site for the screening of colonies.

Genomic DNA preparation

Genomic DNA from mESCs was obtained by harvesting cells using 0.1% Trypsin (Thermo Fisher) and subsequent centrifugation at 500 rpm for 5 min for pellet formation. The cell pellet was resuspended in Quick-Extract (Lucigen) according to manufacturer's instructions. Genomic DNA was stored at 4°C for downstream applications or at -20°C until further usage.

To obtain genomic DNA from flies, a single fly or fly leg was lysed in Squishing buffer (Tris-HCL pH 8.2 20 mM, EDTA 1mM, NaCl 25 mM; Carl Roth) with freshly added Proteinase K (Promega) to a final concentration of 200 µg/ml. DNA was extracted by incubating the samples at 37°C for 30 min, followed by proteinase K inactivation at 95°C for 5 min.

Fluorescence activated cell sorting (FACS)

The used Cas9 plasmid (pSpCas9n(BB)-2A-GFP) (PX461) co-expresses GFP, which we used as a selection tool for transfected cells. Transfected mESCs were additionally stained with propidium iodide to test for viability (Thermo Fisher) and Hoechst dye to assess chromosomal quantity (Thermo Fisher) according to manufacturer's instructions. One day after transfection, cells were single-cell-sorted (for haploidy and GFP-positivity) on 96-well plates with the BD FACSaria Fusion at the FACS and Imaging Core Facility at the Max Planck Institute for Biology of Ageing (MPI-Age). Cells were grown for 10 days after which the single clones were restriction reactions that revealed a positive edit were genotyped.

Cell stress assays (tunicamycin and H_20_2)

The WST-1 assay for cell proliferation and viability (Sigma) was used to measure normal cell growth and response to stressors, i.e. tunicamycin and H_2O_2. To this end, cells were plated at a confluence of 10,000 cells/96-well in quadruplicates and stressors were added in appropriate concentrations after allowing the cells to settle for 2 h. The next day, WST-1 labelling reagent was added according to manufacturer's instructions and the spectrophotometric absorbance (A_{440} nm- A_{690} nm) was measured with a plate reader Infinite 200 (Tecan, Männedorf, Switzerland). Cell viability was normalised to the respective untreated controls.

Fly work

Fly husbandry

Fly stocks **(Table EV6)** were kept at 25°C on a 12 h light/dark cycle and fed a standard sugar/yeast/agar diet (1x SYA). The standard 1x SYA diet contained 5% sugar, 10% yeast, 1.5 % agar, 0.3% nipagin (10% in EtOH) and 0.03% propionic acid (MP Biologicals). In all experiments, female and male flies were reared at controlled larval densities and allowed to mate for 48 h ("once-mated") before each experiment.

Generation of transgenic fly lines

For the generation of the $Nf1^{Phe1148Leu}$ fly, two gRNAs targeting the *Nf1* locus (**Table EV4**) were cloned in a *pCFD4* plasmid, along with a repair template containing the desired mutation with the Gibson Assembly kit (NEB). The *Nf1* donor construct contained the following elements: left homologous arm (512 bp); PAM sites (2) and the mutation of interest; right homologous arm (727 bp). These fragments were amplified from the BAC clone (BACR02E09) and cloned into a *pOT2* vector. Embryos of flies expressing *Cas9* under the ubiquitous actin promoter were injected with 300 ng/µl DNA. PCR screening targeting the restriction site was used to identify positive flies and the correct introduction of the point mutation was confirmed with Sanger Sequencing. The positive $Nf1^{Phe1148Leu}$ fly line was backcrossed for 6 generations into the w^{Dah} background to get rid of possible off-target mutations.

Developmental assay and adult body weight

For developmental time analysis, flies were allowed to lay eggs for 6 h, and these were then transferred to vials at a density of 25 per vial (n_{vials} = 8-10). The number of hatching flies was noted down 2-3 times a day. For body weight measurements of adult flies, 20 age-matched flies were anaesthetized with CO2 and weighed in pairs of two.

Lifespan and fecundity assay

For lifespan assays, once-mated flies were sorted into vials 48 h post eclosion (20 flies per vial, n_{vials} = 8-10). Every other day, flies were transferred to fresh vials and deaths scored. Survival analysis was performed in two independent experiments and the raw lifespan data is provided in **Dataset EV1**. Data was analysed using log-rank and Cox regression where appropriate. For fecundity assays, once-mated female flies were transferred into vials (5 flies per vial, n_{vials} = 8-

10) and the number of eggs was counted using a hand counter once a week for the course of four weeks.

Climbing assay

Half an hour prior to the experiment, flies were placed in plastic climbing assay tubes for acclimation. Subsequently, flies were transferred to vial one of the six-compartment climbing apparatus and tapped down to the bottom of the vial. In this apparatus, flies are allowed to climb to the upper vial ranging a distance of 15 cm for 20 sec. After 20 sec, flies in the upper vial are transferred into the second vial and tapped down. This procedure is repeated until the sixth vial is reached. The climbing index (CI) was calculated based on the number of flies in each vial (lowest = 0 = all flies in vial one, highest = 1 = all flies in vial six). Area under the curve was calculated for the different conditions and then compared to wildtype flies using a one-way ANOVA.

Protein extraction and western blotting

Cells (500,000) and fly heads (n = 12-15) were counted or weighed in desired amounts. Before protein isolation, cells were washed twice with cold PBS (Sigma) after which 100-300 µl RIPA buffer was added (10 ml RIPA Buffer (Thermo Fisher), one cOMPLETE EDTA and one PhosSTOP tablet (Roche, Basel, Switzerland)) to the samples on ice. Cells were harvested using a cell scraper. The suspension was sonicated for 10 sec with 2% pulses and centrifuged at 14.000 rpm at 4°C. Supernatant was transferred to a 1.5 ml tube and stored at -80°C until usage. Fly heads were homogenised in RIPA buffer using a hand homogenizer. After centrifugation, the samples were sonicated in a water bath for 10 min and centrifuged at 13,000 rpm at 4°C. The supernatant was subsequently transferred to new vials. Protein concentration was determined using the BCA Protein Assay Kit (Thermo Fisher) and samples were diluted accordingly. Laemmli Buffer (100 mM Tris pH 6.8, 20% glycerol, 4% SDS, (Carl Roth, Germany)) and 5% β- mercaptoethanol (Sigma) were added to the samples after which they were heated to 95°C for 5 min.

Equal amounts of proteins (25 µg) were loaded and separated at 100-150 Volt for 90 min, using pre-stained SDS-PAGE gels (Bio-Rad). Stain-Free gels were activated with UV light for 2.5 min with the ChemiDocImager (Bio-Rad) before transferring them onto a 0.45 µm nitrocellulose membrane (GE Healthcare, Illinois, United States) at 100 V for 1 h. After the transfer, Stain-Free images were captured using the ChemiDocImager (Bio-Rad). The

membrane was blocked using 5% non-fat dry milk powder/TBST for one hour and incubated with primary antibodies **(Table EV7)** at 4°C overnight. Afterwards, the membranes were washed three times for 15 min each and the appropriate Horseradish peroxidase (HRP) coupled secondary antibody (1:10,000) was added (ThermoFisher). For signal development, ECL Select Western Blotting Detection Reagent (GE Healthcare) was added and images were captured using the ChemiDocImager (Bio-Rad).

LC-MS/MS of mESCs

Protein extraction

mESCs were grown at 500,000, pellets collected by trypsinization and washed three times with PBS (Sigma). The cell pellet was resuspended in 20 µl lysis buffer. The mixture was heated to 95°C for 10 min and sonicated in a Bioruptor (Diagenode, Liege, Belgium) (30 sec sonication, 30 sec breaks, 10 cycles). The lysate was centrifuged at 20,000x g for 10 min and transferred to new tubes. Protein concentrations were measured with NanoDrop (Thermo Fisher) and 300 µg diluted ten times with 20 mM Tris and digested with trypsin 1:200 overnight. The digestion was stopped the next morning by adding 100% formic acid (FA) and samples cleared by centrifugation at 20,000x g for 10 min.

Peptide cleaning

Peptide cleaning was performed with house-made 30 µg C18-SD StageTips. In brief, these tips were wet with methanol, then 40% acetonitrile/0.1% FA and equilibrated with 0.1% FA by table centrifugations of 1-2 min without letting the tips dry in between these steps. The total protein digest was then loaded in 0.1% FA and washed with 0.1% FA. Final elution was done with 100 µl 40% acetonitrile/0.1% FA at 300x g for 4 min and elutes dried in a SpeedVac at 45°C for 35 min. The digest was resuspended in 20 µl 0.1% FA and concentrations measured with NanoDrop (Thermo Fisher). 4 µg of peptides were used for subsequent TMT labelling.

Tandem Mass Tag (TMT) Pro labelling and fractionation

The peptides were reconstituted in 0.1 M triethylammonium bicarbonate buffer (Sigma Aldrich) and TMT Pro labelling done according to manufacturer's instructions (Thermo Fisher). The ratio of peptides to TMT Pro reagent was 1:20. Labelled peptides were pooled, dried and resuspended in 200 µl 0.1% FA. These were then fractionated on a 1 mm x 150 mm ACQUITY column, packed with 130 Å, 1.7 µm C18 particles (Waters, Massachusetts, United

States), using an Ultimate 3000 UHPLC (Thermo Fisher). Peptides were separated at a flow of 30 µL/min with an 88 min segmented gradient from 1% to 50% buffer B for 85 min and from 50% to 95% buffer A for 3 min. Buffer A contained 5% acetonitrile, 10 mM ammonium bicarbonate, buffer B contained 80% acetonitrile, 10mM ammonium bicarbonate. Fractions were collected every three minutes, pooled and dried in a SpeedVac.

LC-MS/MS analysis

Dried fractions were resuspended in 0.1% FA and separated on a 50 cm, 75 µm Acclaim PepMap column (Thermo Fisher) and analysed on a Orbitrap Lumos Tribrid mass spectrometer (Thermo Fisher) equipped with a FAIMS device (Thermo Fisher). The FAIMS device was operated in two compensation voltages, -50 V and -70 V. Peptide separations were performed on an EASY-nLC1200 using a 90 min linear gradient from 6% to 31% buffer. Buffer A contained 0.1% FA, buffer B contained 0.1% FA and 80% acetonitrile. The analytical column was operated at 50°C. Raw files were split based on the FAIMS compensation voltage using FreeStyle (Thermo Fisher). The final data was analysed using MaxQuant [73].

Statistics

Data were analysed statistically using GraphPad Prism 9.5.0. The value of α was 0.05, and data were expressed as *P < 0.05; **P < 0.01; ***P < 0.001; ****P < 0.0001. A Student's t-test was used when comparison was made across only two groups. Across groups comparisons were made using one-way ANOVA and between groups using a Tukey post hoc test. Repeated measures two-way ANOVA was used to analyse climbing ability with Tukey's post hoc test for multiple correction to test for differences at specific ages. R 4.2.2 was used for the survival and proteomic analyses. Survivorship was analysed using log rank test and Cox proportional hazard analysis using the following R packages "survival" and "survminer". The proteomic data was processed and analysed using a custom-made pipeline based on the R packages "edgeR", "VennDiagram", "clusterProfiler" (over-representation analyses), "msigdbr", and "ggplot2". All error bars correspond to standard deviation except for stress assays where standard error of the mean is reported.

Data availability

The code used for the analyses of the proteomics data is available upon request from the corresponding author Joris Deelen. The raw lifespan data is provided as a supplementary dataset (**Dataset EV1**). The proteomics data produced in this study is available in the PRoteomics IDEntifications Database (http://www.ebi.ac.uk/pride/archive/projects/PXDXXXXXX).

Acknowledgments

We thank the study participants of the Leiden Longevity Study. We thank the Proteomics and FACS and Imaging Core Facilities of the MPI-Age for outstanding technical help and advice. We thank Jaqueline Eßer for assistance in transgenic fly generation and Isabell Brusius for assistance in proteomics analysis. **Figure 1** and **Figure 4A-B** were created with BioRender.com. This project has received funding from the European Research Council (ERC) under the European Union's Horizon 2020 (grant agreement n° 741989) and Horizon Europe (ElucidAge, 101041331) research and innovation programmes. Views and opinions expressed are however those of the author(s) only and do not necessarily reflect those of the European Union or the European Research Council Executive Agency. Neither the European Union nor the granting authority can be held responsible for them.

Author contributions

Helena Hinterding: Methodology; investigation; formal analysis; visualization; writing – original draft; writing – review and editing.
Maarouf Baghdadi: Conceptualization; methodology; investigation; visualization; writing – original draft; writing – review and editing.
Thies Gehrmann: Investigation; formal analysis.
Pasquale Putter: Investigation; formal analysis; validation; writing – review and editing.
Nico Lakenberg: Investigation.
Erik B. van den Akker: Supervision; methodology.
P. Eline Slagboom: Conceptualization; resources; supervision; funding acquisition; writing – review and editing.

Joris Deelen: Conceptualization; resources; supervision; methodology; investigation; formal analysis; funding acquisition; writing – original draft; writing – review and editing.
Linda Partridge: Conceptualization; resources; supervision; funding acquisition; writing – review and editing.

Disclosures and competing interests statement

The authors declare no competing interests.

References

1. Partridge, L., Deelen, J. & Slagboom, P. E. Facing up to the global challenges of ageing. *Nature* **561**, 45–56 (2018).
2. Oeppen, J. & Vaupel, J. W. Demography. Broken limits to life expectancy. *Science* **296**, 1029–1031 (2002).
3. Crimmins, E. M. Lifespan and healthspan: Past, present, and promise. *Gerontologist* **55**, 901–911 (2015).
4. Andersen, S. L., Sebastiani, P., Dworkis, D. A., Feldman, L. & Perls, T. T. Health span approximates life span among many supercentenarians: compression of morbidity at the approximate limit of life span. *J. Gerontol. A Biol. Sci. Med. Sci.* **67**, 395–405 (2012).
5. Christensen, K., McGue, M., Petersen, I., Jeune, B. & Vaupel, J. W. Exceptional longevity does not result in excessive levels of disability. *Proc. Natl. Acad. Sci. U. S. A.* **105**, 13274–13279 (2008).
6. Baghdadi, M., Karasik, D. & Deelen, J. Genetic control of aging. in *Encyclopedia of Gerontology and Population Aging* 2018–2025 (Springer International Publishing, 2021).
7. van den Berg, N. *et al.* Longevity around the turn of the 20th century: Life-long sustained survival advantage for parents of today's nonagenarians. *J. Gerontol. A Biol. Sci. Med. Sci.* **73**, 1295–1302 (2018).
8. Montesanto, A. *et al.* The genetic component of human longevity: analysis of the survival advantage of parents and siblings of Italian nonagenarians. *Eur. J. Hum. Genet.* **19**, 882–886 (2011).
9. Perls, T. T. *et al.* Life-long sustained mortality advantage of siblings of centenarians. *Proc. Natl. Acad. Sci. U. S. A.* **99**, 8442–8447 (2002).
10. Willcox, B. J., Willcox, D. C., He, Q., Curb, J. D. & Suzuki, M. Siblings of Okinawan centenarians share lifelong mortality advantages. *J. Gerontol. A Biol. Sci. Med. Sci.* **61**, 345–354 (2006).
11. Schoenmaker, M. *et al.* Evidence of genetic enrichment for exceptional survival using a family approach: the Leiden Longevity Study. *Eur. J. Hum. Genet.* **14**, 79–84 (2005).
12. Wijsman, C. A. *et al.* Familial longevity is marked by enhanced insulin sensitivity. *Aging Cell* **10**, 114–121 (2011).
13. Vaarhorst, A. A. M. *et al.* Lipid metabolism in long-lived families: the Leiden Longevity Study. *Age (Dordr.)* **33**, 219–227 (2011).
14. Deelen, J. *et al.* Employing biomarkers of healthy ageing for leveraging genetic studies into human longevity. *Exp. Gerontol.* **82**, 166–174 (2016).
15. van den Berg, N. *et al.* Longevity defined as top 10% survivors and beyond is transmitted as a quantitative genetic trait. *Nat. Commun.* **10**, 35 (2019).
16. Deelen, J. *et al.* A meta-analysis of genome-wide association studies identifies multiple longevity genes. *Nat. Commun.* **10**, 3669 (2019).
17. Sebastiani, P. *et al.* Four genome-wide association studies identify new extreme longevity variants. *J. Gerontol. A Biol. Sci. Med. Sci.* **72**, 1453–1464 (2017).
18. Liu, X. *et al.* Integrated genetic analyses revealed novel human longevity loci and reduced risks of multiple diseases in a cohort study of 15,651 Chinese individuals. *Aging Cell* **20**, e13323 (2021).
19. Auer, P. L. & Lettre, G. Rare variant association studies: considerations, challenges and opportunities. *Genome Med.* **7**, 16 (2015).
20. Moore, S. R. Commentary: What is the case for candidate gene approaches in the era of high-throughput

genomics? A response to Border and Keller (2017). *J. Child Psychol. Psychiatry* **58**, 331–334 (2017).

21. Baghdadi, M., Hinterding, H. M., Partridge, L. & Deelen, J. From mutation to mechanism: deciphering the molecular function of genetic variants linked to human ageing. *Brief. Funct. Genomics* **21**, 13–23 (2022).
22. Gonzalez, B. *et al.* High-throughput sequencing analysis of nuclear-encoded mitochondrial genes reveals a genetic signature of human longevity. *GeroScience* **45**, 311–330 (2023).
23. Ryu, S. *et al.* Genetic signature of human longevity in PKC and NF-κB signaling. *Aging Cell* **20**, e13362 (2021).
24. Simon, M. *et al.* A rare human centenarian variant of SIRT6 enhances genome stability and interaction with Lamin A. *EMBO J.* **42**, e113326 (2023).
25. Zhang, Z. D. *et al.* Genetics of extreme human longevity to guide drug discovery for healthy ageing. *Nat. Metab.* **2**, 663–672 (2020).
26. Wasylyk, B., Hagman, J. & Gutierrez-Hartmann, A. Ets transcription factors: nuclear effectors of the Ras-MAP-kinase signaling pathway. *Trends Biochem. Sci.* **23**, 213–216 (1998).
27. Fabrizio, P. *et al.* SOD2 functions downstream of Sch9 to extend longevity in yeast. *Genetics* **163**, 35–46 (2003).
28. Okuyama, T. *et al.* The ERK-MAPK pathway regulates longevity through SKN-1 and insulin-like signaling in Caenorhabditis elegans. *J. Biol. Chem.* **285**, 30274–30281 (2010).
29. Slack, C. *et al.* The Ras-Erk-ETS-Signaling Pathway Is a Drug Target for Longevity. *Cell* **162**, 72–83 (2015).
30. Borrás, C. *et al.* RasGrf1 deficiency delays aging in mice. *Aging* **3**, 262–276 (2011).
31. Cargnello, M. & Roux, P. P. Activation and function of the MAPKs and their substrates, the MAPK-activated protein kinases. *Microbiol. Mol. Biol. Rev.* **76**, 496–496 (2012).
32. Raman, M., Chen, W. & Cobb, M. H. Differential regulation and properties of MAPKs. *Oncogene* **26**, 3100–3112 (2007).
33. van den Akker, E. B. *et al.* Uncompromised 10-year survival of oldest old carrying somatic mutations in DNMT3A and TET2. *Blood* **127**, 1512 (2016).
34. Kircher, M. *et al.* A general framework for estimating the relative pathogenicity of human genetic variants. *Nat. Genet.* **46**, 310–315 (2014).
35. Boomsma, D. I. *et al.* The Genome of the Netherlands: design, and project goals. *Eur. J. Hum. Genet.* **22**, 221–227 (2014).
36. Ran, F. A. *et al.* Genome engineering using the CRISPR-Cas9 system. *Nat. Protoc.* **8**, 2281–2308 (2013).
37. Elling, U. *et al.* A reversible haploid mouse embryonic stem cell biobank resource for functional genomics. *Nature* **550**, 114–118 (2017).
38. Martinez-Lopez, N., Athonvarangkul, D., Mishall, P., Sahu, S. & Singh, R. Autophagy proteins regulate ERK phosphorylation. *Nat. Commun.* **4**, 2799 (2013).
39. Masaki, T. *et al.* Activation of the ERK pathway precedes tubular proliferation in the obstructed rat kidney. *Kidney Int.* **63**, 1256–1264 (2003).
40. Mitic, M., Lukic, I., Bozovic, N., Djordjevic, J. & Adzic, M. Fluoxetine signature on hippocampal MAPK signalling in sex-dependent manner. *J. Mol. Neurosci.* **55**, 335–346 (2015).
41. Pandit, B. *et al.* Gain-of-function RAF1 mutations cause Noonan and LEOPARD syndromes with hypertrophic cardiomyopathy. *Nat. Genet.* **39**, 1007–1012 (2007).

42. Masgras, I. *et al.* Absence of neurofibromin induces an oncogenic metabolic switch via mitochondrial ERK-mediated phosphorylation of the chaperone TRAP1. *Cell Rep.* **18**, 659–672 (2017).
43. Razzaque, M. A. *et al.* Germline gain-of-function mutations in RAF1 cause Noonan syndrome. *Nat. Genet.* **39**, 1013–1017 (2007).
44. Darling, N. J. & Cook, S. J. The role of MAPK signalling pathways in the response to endoplasmic reticulum stress. *Biochim. Biophys. Acta* **1843**, (2014).
45. Guyton, K. Z., Liu, Y., Gorospe, M., Xu, Q. & Holbrook, N. J. Activation of mitogen-activated protein kinase by H2O2. Role in cell survival following oxidant injury. *J. Biol. Chem.* **271**, (1996).
46. Rezatabar, S. *et al.* RAS/MAPK signaling functions in oxidative stress, DNA damage response and cancer progression. *J. Cell. Physiol.* **234**, (2019).
47. Son, Y. *et al.* Mitogen-Activated Protein Kinases and Reactive Oxygen Species: How Can ROS Activate MAPK Pathways? *J. Signal Transduct.* **2011**, (2011).
48. Walker, J. A. *et al.* Reduced growth of Drosophila neurofibromatosis 1 mutants reflects a non-cell-autonomous requirement for GTPase-Activating Protein activity in larval neurons. *Genes Dev.* **20**, 3311–3323 (2006).
49. Fowler, K. & Partridge, L. A cost of mating in female fruitflies. *Nature* **338**, 760–761 (1989).
50. Partridge, L. & Barton, N. H. Optimality, mutation and the evolution of ageing. *Nature* **362**, 305–311 (1993).
51. Rhodenizer, D., Martin, I., Bhandari, P., Pletcher, S. D. & Grotewiel, M. Genetic and environmental factors impact age-related impairment of negative geotaxis in Drosophila by altering age-dependent climbing speed. *Exp. Gerontol.* **43**, 739–748 (2008).
52. Ikeyama, S., Kokkonen, G., Shack, S., Wang, X.-T. & Holbrook, N. J. Loss in oxidative stress tolerance with aging linked to reduced extracellular signal-regulated kinase and Akt kinase activities. *FASEB J.* **16**, 1–16 (2002).
53. Tresini, M., Lorenzini, A., Torres, C. & Cristofalo, V. J. Modulation of replicative senescence of diploid human cells by nuclear ERK signaling. *J. Biol. Chem.* **282**, 4136–4151 (2007).
54. Hüser, M. *et al.* MEK kinase activity is not necessary for Raf-1 function. *EMBO J.* **20**, 1940–1951 (2001).
55. Mercer, K. *et al.* A-Raf and Raf-1 work together to influence transient ERK phosphorylation and Gl/S cell cycle progression. *Oncogene* **24**, 5207–5217 (2005).
56. Yamaguchi, O. *et al.* Cardiac-specific disruption of the c-raf-1 gene induces cardiac dysfunction and apoptosis. *J. Clin. Invest.* **114**, 937–943 (2004).
57. Copeland, J. M. *et al.* Extension of Drosophila life span by RNAi of the mitochondrial respiratory chain. *Curr. Biol.* **19**, 1591–1598 (2009).
58. Lapointe, J. & Hekimi, S. Early mitochondrial dysfunction in long-lived Mclk1+/- mice. *J. Biol. Chem.* **283**, 26217–26227 (2008).
59. Lee, S.-J., Hwang, A. B. & Kenyon, C. Inhibition of respiration extends C. elegans life span via reactive oxygen species that increase HIF-1 activity. *Curr. Biol.* **20**, 2131–2136 (2010).
60. Harshman, L. G., Moore, K. M., Sty, M. A. & Magwire, M. M. Stress resistance and longevity in selected lines of Drosophila melanogaster. *Neurobiol. Aging* **20**, (1999).
61. Johnson, T. E. *et al.* Longevity genes in the nematode Caenorhabditis elegans also mediate increased resistance to stress and prevent disease. *J. Inherit. Metab. Dis.* **25**, 197–206 (2002).

62. Lithgow, G. J. & Walker, G. A. Stress resistance as a determinate of C. elegans lifespan. *Mech. Ageing Dev.* **123**, (2002).
63. Murakami, S. Stress resistance in long-lived mouse models. *Exp. Gerontol.* **41**, (2006).
64. Tong, J. J., Schriner, S. E., McCleary, D., Day, B. J. & Wallace, D. C. Life extension through neurofibromin mitochondrial regulation and antioxidant therapy for neurofibromatosis-1 in Drosophila melanogaster. *Nat. Genet.* **39**, (2007).
65. Gonzalez, M. A. & Bernad, A. Characteristics of Adult Stem Cells. *Stem Cell Transplantation* 103–120 (2012).
66. Kroef, V. *et al.* GFPT2/GFAT2 and AMDHD2 act in tandem to control the hexosamine pathway. *Elife* **11**, (2022).
67. Paquet, D. *et al.* Efficient introduction of specific homozygous and heterozygous mutations using CRISPR/Cas9. *Nature* **533**, 125–129 (2016).
68. Lee, S., Abecasis, G. R., Boehnke, M. & Lin, X. Rare-variant association analysis: study designs and statistical tests. *Am. J. Hum. Genet.* **95**, 5–23 (2014).
69. McLaren, W. *et al.* The Ensembl Variant Effect Predictor. *Genome Biol.* **17**, 122 (2016).
70. Deelen, J. *et al.* Genome-wide association meta-analysis of human longevity identifies a novel locus conferring survival beyond 90 years of age. *Hum. Mol. Genet.* **23**, 4420–4432 (2014).
71. Abecasis, G. R., Cherny, S. S., Cookson, W. O. & Cardon, L. R. Merlin--rapid analysis of dense genetic maps using sparse gene flow trees. *Nat. Genet.* **30**, 97–101 (2002).
72. Ran, F. A. *et al.* Double nicking by RNA-guided CRISPR Cas9 for enhanced genome editing specificity. *Cell* **154**, 1380–1389 (2013).
73. Cox, J. & Mann, M. MaxQuant enables high peptide identification rates, individualized p.p.b.-range mass accuracies and proteome-wide protein quantification. *Nat. Biotechnol.* **26**, 1367–1372 (2008).